Article

Zhuyu Pill Alleviates Nonalcoholic Fatty Liver Disease by Regulating Bile Acid Metabolism through the Gut−Liver Axis

Lu Xu, Kunhe Xu, Peiyu Xiong, Chun Zhong, Xiaobo Zhang, Rui Gao, Xin Zhou,* and Tao Shen*

Cite This: *ACS Omega* 2023, 8, 29033−29045

Read Online

| ACCESS | | Metrics & More | | Article Recommendations | | Supporting Information |

ABSTRACT: Aim. The prevalence of nonalcoholic fatty liver disease (NAFLD) is increasing worldwide, but there are currently limited treatment options available. Therefore, it is necessary to research new treatment strategies. Zhuyu Pill (ZYP) is a well-known herbal recipe consisting of Huanglian (Coptidis rhizoma) and Wuzhuyu (Evodiae Fructus) that has been clinically used to treat NAFLD. This study aimed to investigate the impact of ZYP on NAFLD induced by a high-fat diet (HFD) and to identify its potential mechanism. Methods. In this investigation, we used ZYP to treat a mouse model of NAFLD induced by an HFD. We conducted various analyses including assessment of serum biochemical indices, histological evaluation, fecal metabonomics analysis, western blot, and quantitative real-time polymerase chain reaction. Results. ZYP effectively improved blood lipid levels and reduced inflammatory response in HFD mice, while also alleviating liver cell damage and lipid accumulation. Additionally, ZYP influenced the fecal bile acid (BA) metabolism profiles of HFD mice by inhibiting the signal transduction of ileal farnesoid X receptor (FXR) fibroblast growth factor 15 (FGF15), enhancing the expression of cytochrome P450 family 7 subfamily A member 1(CYP7A1), promoting BA synthesis and increasing the metabolic elimination of cholesterol. Conclusion. ZYP shows promise as a potential treatment for alleviating NAFLD by modulating BA metabolism through the FXR-FGF15-CYP7A1 pathway.

1. INTRODUCTION

Nonalcoholic fatty liver disease (NAFLD) has emerged as the most prevalent chronic liver disease and a significant global health concern, affecting approximately one-quarter of the world's population.[1,2] NAFLD is a complex systemic disorder characterized by the accumulation of lipids in the liver, lipid toxicity, inflammation, insulin resistance, and dysbiosis of the gut microbiome.[3] The economic burden of NAFLD is substantial, with an estimated annual cost of €35 billion in Europe-4 countries (Britain, France, Germany, and Italy) and approximately $103 billion in the United States.[4] Currently, neither the US Food and Drug Administration nor the European Medicines Agency has authorized drug therapy for NAFLD. Additionally, NAFLD patients currently lack access to any medications that can reduce their risk of significant liver complications or serious adverse cardiovascular events.[5−9] The problem of identifying effective treatments for NAFLD is becoming increasingly apparent as the clinical and financial costs associated with the condition continue to rise. Traditional Chinese medicine (TCM) has shown efficacy in treating NAFLD.[10,11] TCM substances have multiple components and exert multiple pharmacological effects that align with the complex pathophysiology of NAFLD.[12] These substances have been used for thousands of years in Asia to safely treat liver disorders and other ailments.

Huaglian (Coptidis rhizoma)−Wuzhuyu (Evodiae Fructus) is a well-known herb pair combination (HYHP) that is commonly used for the treatment of liver, gallbladder, and digestive diseases.[13−15] Recent research has revealed that HYHP contains several active chemicals, including berberine and evodiamine, which have diverse pharmacological effects,

such as anti-inflammatory, anti-fibrotic, barrier protection, flora regulation, and lipid-lowering properties.[16−18] Zhuyu Pill (ZYP, Huanglian and Wuzhuyu in a 1:1 ratio, g/g) is a traditional HYPY formula. Previous studies have demonstrated that ZYP effectively reduces inflammation and hepatic steatosis in mice by suppressing the NLRP3 inflammasome.[19] ZYP significantly improved the biochemical parameters, liver tissue damage, metabolic spectrum, and ANIT alterations in rats with cholestasis.[20,21]

Bile acids (BAs) are byproducts of cholesterol metabolism and have various biological effects on NAFLD biology. These effects include regulating liver lipid drive, cell damage, inflammation, fibrosis, insulin sensitivity, and glucose processing.[22] BA synthesis is regulated by a negative feedback signal involving overexpression of the farnesoid X receptor (FXR), which is found in many tissues but is most abundant in the intestine and liver. When FXR is overexpressed in the intestine, it causes the transcription of fibroblast growth factor 15 (FGF15, human FGF19), which goes to the liver through the portal vein. FGF15 interacts with fibroblast growth factor receptor 4 (FGFR4) in the liver, inhibiting the expression of cytochrome P450 family 7 subfamily A member 1 (CYP7A1) and reducing BA synthesis.[23−25]

	1-7 days	8 days-64 days	65 days
CON	acclimate	normal diet	distilled water	sacrifice
HFD	acclimate	HFD	distilled water	sacrifice
ATO	acclimate	HFD	1.5mg/kg ATO	sacrifice
ZYP-L	acclimate	HFD	0.75g/kg ZYP	sacrifice
ZYP-M	acclimate	HFD	1.5g/kg ZYP	sacrifice
ZYP-H	acclimate	HFD	3g/kg ZYP	sacrifice

Figure 1. Animal experiment design diagram.

The objective of this study is to determine if ZYP can prevent NAFLD induced by a high-fat diet (HFD) by modifying BA metabolism. To induce hepatic steatosis, mice were fed an HFD containing cholesterol (1%), propylthiouracil (0.2%), egg yolk powder (5%), sodium taurocholate (1%), lard (8%), and basic diet (84.8%) for 8 weeks, along with varying doses of ZYP. Targeted metabolomics was used to analyze the fecal BA profiles of mice on a normal diet, HFD, and ZYP-fed mice. Furthermore, we investigated the role of BAs in NAFLD and found that certain BAs decreased the expression of FXR in the intestine, blocked the FGF15/FGFR4 pathway, activated CYP7A1 expression in the liver, increased BA production and excretion, and significantly improved lipid metabolism and inflammation.

2. MATERIALS AND METHODS

2.1. Animals. The Ethics Committee of Hospital of Chengdu University of TCM (Chengdu, China) approved the experiment protocols under license number 2021DL-001. Chengdu Dashuo Biotechnology Co., Ltd. donated 36 male C57BL/6 mice (6−8 weeks old, 18−20 g) (Chengdu, China; certificate no. SCXK-Chuan 2015-030). All experimental animals were maintained in an SPF environment with continuous circumstances of a 12 h/12 h light/dark cycle at 22−23 °C and 55−60% humidity.

2.2. Preparation of ZYP. ZYP is composed of Huanglian (Coptidis rhizoma) and Wuzhuyu (Evodiae Fructus) in a ratio of 1:1. Beijing Tongrentang CO., LTD. was the source of all herbs (Chengdu, China). ZYP was made in the following way: weighed together, Huanglian and Wuzhuyu were submerged for 6 h in 120 mL of distilled water (1:10). Then, these samples underwent two 45 min boils. High-performance liquid chromatography (HPLC) chromatographic analysis was done to identify the active ingredients in ZYP formulations. In our prior paper, the HPLC analytical process and distinctive chromatogram of ZYP were discussed.[20]

2.3. Animal Experiments. Figure 1 displays the design schematic for the animal experiment. Animals were randomly apportioned to one of six groups ($n = 6$) after a week of acclimatization: control (CON), HFD, ZYP—low dosage (ZYP-L), ZYP—medium dose (ZYP-M), ZYP—high dose (ZYP-H), and Atorvastatin (ATO) groups. Serum total cholesterol (TC) levels were measured in mouse tail vein blood; there was no difference between groups for serum TC levels or body weight (Supporting Information Figure S1). In the CON group, the mice were given a normal meal and distilled water through gavage. The mice in the HFD group were administered distilled water and HFD through gavage daily. For the low dose group, the maximum clinical dose recommended by Chinese Pharmacopoeia (2020 edition) was used, which was ZYP-L (0.75 g/kg) for mice.[19] The ZYP

treatment groups were given HFD along with daily dosages of ZYP, with the dosages being 0.75 g/kg (ZYP-L), 1.5 g/kg (ZYP-M), and 3 g/kg (ZYP-H), respectively. In the ATO group, the mice received daily ATO gavage (1.5 mg/kg) along with an HFD.[26]

The HFD used in the study consisted of 8% lard, 1% sodium tauroglycocholate, 5% yolk powder, 0.2% propylthiouracil, 1% cholesterol, and 84.8% normal diet.[27] During the trial, the weight of the mice was measured weekly, and their food consumption was recorded.

2.4. Serum Biochemical Analysis. At 8 weeks, mice were fasted for 12 h and then anesthetized for blood collection. The serum was collected by centrifuging at 3700g at 4 °C for 15 min. Serum TC and serum triglyceride (TG) were measured using enzymatic assay kits (APPLYGEN Co., LTD, Beijing, China). Serum low-density lipoprotein cholesterol (LDL-C) and high-density lipoprotein cholesterol (HDL-C) were measured using enzymatic assay kits (Jiancheng Co., LTD, Nanjing, China). Serum interleukin-6 (IL-6), interleukin-10 (IL-10), and tumor necrosis factor-α (TNF-α) were measured using commercial ELISA kits (Jiancheng Co., LTD, Nanjing, China). Blood Glucose was measured using an assay kit (Solarbio Co., LTD, Beijing, China).

2.5. Liver Histological Analyzes. The hepatic tissues were isolated and fixed in 10% neutral formaldehyde for 24 h. The slices were then dehydrated using a graduated ethanol series before being embedded in paraffin. Hematoxylin−eosin (H&E) was used to stain the embedded wax blocks into 5 m thick slices for morphological analysis.

2.6. Quantitative Real-Time Polymerase Chain Reaction. Total RNA was isolated using the Animal Total RNA Isolation Kit (Fore Gene, Chengdu, China) as directed by the manufacturer. RT EasyTM II (With gDNase) was then used to convert the total RNA to complementary DNA (cDNA) (Fore Gene, Chengdu, China). The CFX Connect Real-time System (BIO-RAD, Singapore) was used for the quantitative real-time polymerase chain reaction (RT-qPCR), which included predenaturation at 95 °C for 30 s, denaturation at 95 °C for 5 s, annealing at 60 °C, and extension for 30 s for a total of 40 cycles. Shanghai Bioengineering Co., Ltd. produced the primers, and the primer sequences are provided in Table 1. The levels of the targeted genes were normalized to the levels of the GAPDH gene, and the data were evaluated using the ΔΔCT analysis method.

2.7. Western Blot Analyses. RIPA buffer (BOSTER Biological Technology Co. Ltd, Wuhan, China) was used to lyse the tissues of the liver and intestine. A BCA protein assay kit (BOSTER Biological Technology Co. Ltd, Wuhan, China) was used to measure the protein concentration. On sodium dodecyl sulfate 10% SDS-PAGE, the same quantities of protein were electrophoresed and then transferred to PVDF

Table 1. Real-Time Fluorescence Quantitative PCR Primer Sequence

gene		primer sequences (5′−3′)
CYP7A1	forward	GGGAATGCCATTTACTTGGATC
	reverse	TATAGGAACCATCCTCAAGGTG
FGF15	forward	AGACGATTGCCATCAAGGACG
	reverse	GTACTGGTTGTAGCCTAAACAG
FXR	forward	GTTCGGCGGAGATTTTCAATAAG
	reverse	AGTCATTTTGAGTTCTCCAACAC
FGFR4	forward	CTCGATCCGCTTTGGGAATTC
	reverse	CAGGTCTGCCAAATCCTTGTC
GAPDH	forward	CTGCGACTTCAACAGCAACT
	reverse	GAGTTGGGATAGGGCCTCTC

membranes. The membrane was incubated with the primary antibody overnight at 4 °C after being blocked with 5% nonfat dry milk at room temperature. Primary antibodies used were CYP7A1 (1:1000, PB0578, BOSTER, Wuhan, China), FGFR4 (1:1000, BM5163, BOSTER, Wuhan, China), FXR (1:1000, BM5091, BOSTER, Wuhan, China), FGF15 (1:1000, PB1117, BOSTER, Wuhan, China), and GAPDH (1:2000, BM1623, BOSTER, Wuhan, China). After being three times rinsed with TBST solution, the membranes were incubated with HRP-conjugated secondary antibodies (1:5000, BA1054P, BOSTER, Wuhan, China) at room temperature for 2 h. The grayscale values of the gel bands were measured using the ImageJ software.

2.8. BA Analysis. *2.8.1. Metabolite Extraction.* For MP homogenization, the obtained 30 mg samples—5 mice per group—were put in 120 L of ultrapure water that had already been refrigerated. Once the internal standard and 1000 mL of pre-cooled methanol buffer had been added, the mixture was vortexed for 1 min, incubated at −20 °C for 20 min, and centrifuged at 14,000 rcf for 15 min at 4 °C, and the supernatant was vacuum-dried.

2.8.2. Liquid Chromatography−Mass spectrometry Analysis. The metabolites were separated by chromatography using a Waters ACQUITY UPLC I-Class machine (SCIEX, UK). Solvent A (water, 0.1% formic acid) and Solvent B (methanol, 0.1% formic acid) made up the mobile phase. The gradient elution conditions with a flow rate of 300 L/min were as follows: 0−6 min: 60−65% solvent B; 6−13 min: 65−80% solvent B; 13−13.5 min: 80−90% solvent B; and 13.5−15 min: 90% solvent B; and the column temperature was maintained at 45 °C.

A negative ion mode 5500 QTRAP mass spectrometer (AB SCIEX) was used for the mass spectrometry (MS) study. The following are the 5500 QTRAP ESI source conditions: on spary voltage floating (ISVF): −4500 V; ion source gas1 (Gas1): 55; ion source gas2 (Gas2): 55; curtain gas (CUR): 40; and source temperature: 550 °C. In the MRM mode, the transition under test is found.

2.8.3. Metabolomics Data Processing. Multiquant software was used to obtain retention times and chromatographic peak regions. BA standards were used to adjust retention periods for metabolite identification. All samples were combined in the same proportions to create QC samples, which were then used to assess the consistency and repeatability of the data.

2.9. Statistical Analysis. All data are expressed as mean ± SD. The software programs GraphPad Prism (GraphPad Software 8.0, La Jolla, CA, USA) and SPSS (IBM SPSS version 22.0, Chicago, IL, USA) were used to statistically analyze the

data. One-way analysis of variance (ANOVA) was used to evaluate statistical significance for the majority of parameters in the intervention group. Statistical significance was defined as a p-value less than 0.05.

3. RESULTS

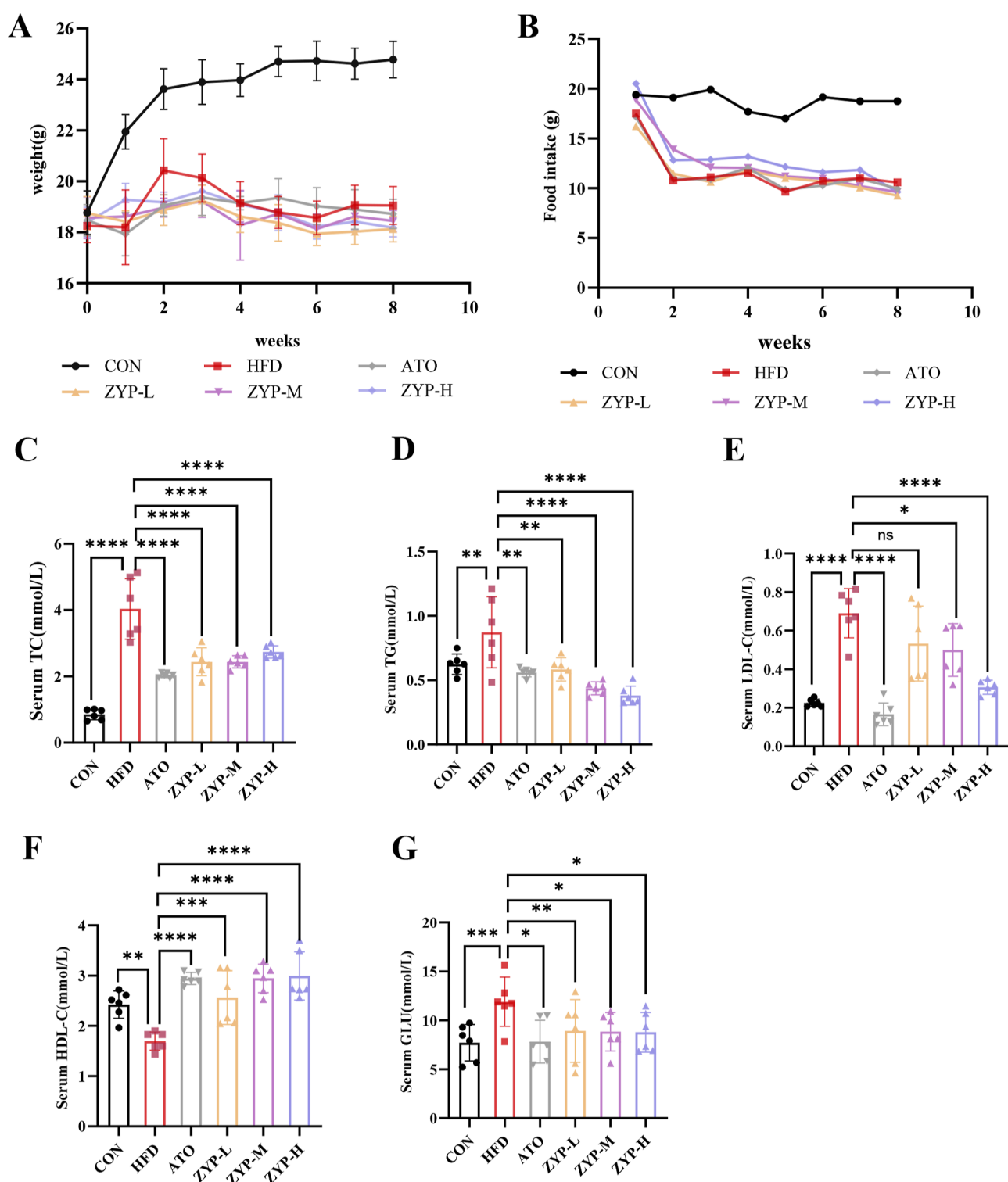**3.1. ZYP Affected Blood Lipid Profiles in NAFLD Mice.** Body weight, food intake, and serum TG, TC, HDL-C, and LDL-C levels were measured in NAFLD mice to evaluate the effects of ZYP. Compared to the CON group, the mice in the HFD group showed a significant decrease in body weight and food intake. However, there were no significant differences in body weight and food intake among the various treatment groups and the HFD group, as well as across the other treatment groups (Figure 2A,B). The ZYP feeding intervention resulted in decreased levels of serum TC, TG, and LDL-C (Figure 2C,E) with increased levels of serum HDL-C (Figure 2F). This indicates that ZYP supplementation effectively reduced dyslipidemia induced by an HFD in mice. NAFLD is a complex systemic disease often associated with impaired glucose metabolism. Compared to the CON group, the HFD group had significantly higher blood glucose levels. However, both ZYP and ATO interventions led to a decrease in blood glucose levels in NAFLD mice (Figure 2G).

3.2. ZYP Alleviates Liver Injury in NAFLD Mice. The livers of mice were removed and imaged. The liver tissues of mice in the CON group appeared as brilliant red, with a smooth surface, obvious edges, and soft texture, as shown in Figure 3A. NAFLD is caused by a high-fat, high-cholesterol diet. The liver tissue of mice in the HFD group showed evident steatosis after being fed an HFD. The pathological abnormalities in the liver tissue of the HFD group were characterized by a dark red color, blunt and thick margins, a somewhat hard texture, and the presence of apparent white fat particles, indicating that HFD increased the development of hepatic steatosis in mice. The pathological alterations observed in the liver tissue of the ZYP and ATO therapy groups were different from those in the HFD group, and there was a significant decrease in the formation of fat particles.

The liver weight index was calculated as the ratio of liver weight to body weight to accurately compare variations in liver pathology among individuals. The liver weight index in the HFD group was significantly higher than in the CON group. However, both the ATO and ZYP treatment groups exhibited a considerable reduction in the liver weight index compared to that in the HFD group (Figure 3C).

We evaluated the pathological alterations in the liver to see if ZYP reduced HFD-induced liver damage. The liver slices of the CON group mice showed no evident pathological alterations and no steatosis, as seen in Figure 3B. The HFD group displayed significant liver steatosis, with ballooning hepatocyte degradation and apparent infiltration of inflammatory cells in the lobular center and portal vein region, confirming the effective creation of the NAFLD model. The fatty degeneration in the ZYP treatment groups was improved to some extent when compared to the HFD group. The pathological section shows that the ZYP-H group improved the most, coming close to the ATO group. The findings demonstrated that ZYP improved liver lipid storage and reduced liver steatosis induced by HFD.

On H&E-stained liver samples, we also performed a histological NAS assessment. As demonstrated in Figure 3D, the HFD group had considerably better NAS scoring system

Figure 2. ZYP affected blood lipid profiles in NAFLD mice. (A) Weight change curve during the whole 8 week intervention. (B) Food intake changed during the whole 8 week intervention. (C) Serum TC levels. (D) Serum TG levels. (E) Serum LDL-C levels. (F) Serum HDL-C levels. (G) Serum GLU levels. ****/***/**/*, $P < 0.0001/P < 0.001/P < 0.01/P < 0.05$; ns, not significant.

scores in all categories than the CON group. The NAS scores of mice in the ZYP therapy groups (low, medium, and high) were considerably reduced as compared to those in the HFD group.

3.3. ZYP Reduced Inflammation in NAFLD Mice. Serum cytokine levels were measured to evaluate the role of ZYP in controlling inflammation in NAFLD. As demonstrated

in Figure 4, blood IL-6 and TNF-α levels in the HFD group were considerably higher than in the CON group (Figure 4A,B), whereas serum IL-10 levels were significantly lower (Figure 4C), indicating systemic chronic inflammation. Serum IL-6 and TNF-α levels in the ZYP treatment groups were considerably lower than in the HFD group (Figure 4A,B), and serum IL-10 levels were significantly higher (Figure 4C). As a
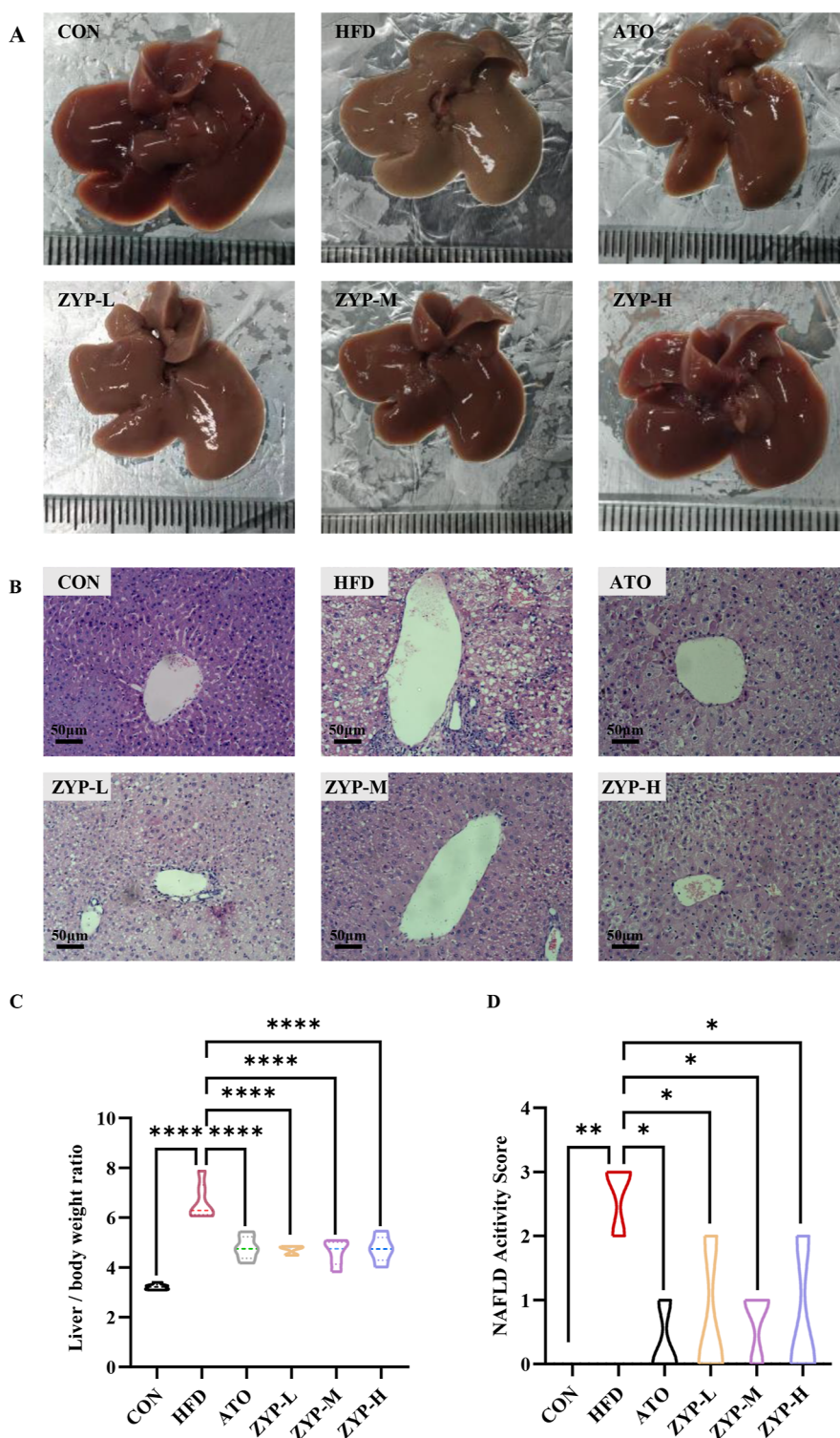
Figure 3. ZYP alleviates liver injury in NAFLD mice. (A) Pathological changes of liver tissue. (B) Representative images of H&E staining of liver sections (50 μm; scale bar). (C) Liver weight index. (D) Results of NAS assessment of H&E stained liver tissue. ****/***/**/*, $P < 0.0001/P < 0.001/P < 0.01/P < 0.05$; ns, not significant.

result, our findings show that ZYP consumption dramatically reduces HFD-induced inflammation in mice.

3.4. ZYP Treats NAFLD by Altering BA Metabolism. To examine the effects of ZYP on HFD mice, fresh fecal samples from each group ($n = 5$) were collected and analyzed by LC–MS. The HFD group had an increase in secondary BAs and free BAs in comparison to the CON group (Figure 5B,C).

In HFD mice, ZYP intervention decreased free BAs and increased conjugated BAs, while increasing primary BAs and decreasing secondary BAs (Figure 5B,A) (Figure 5C,D). The ratio of primary BAs to secondary BAs and the ratio of conjugated BAs to free BAs were both substantially higher after ZYP intervention compared to the HFD group (Figure 5E,F).
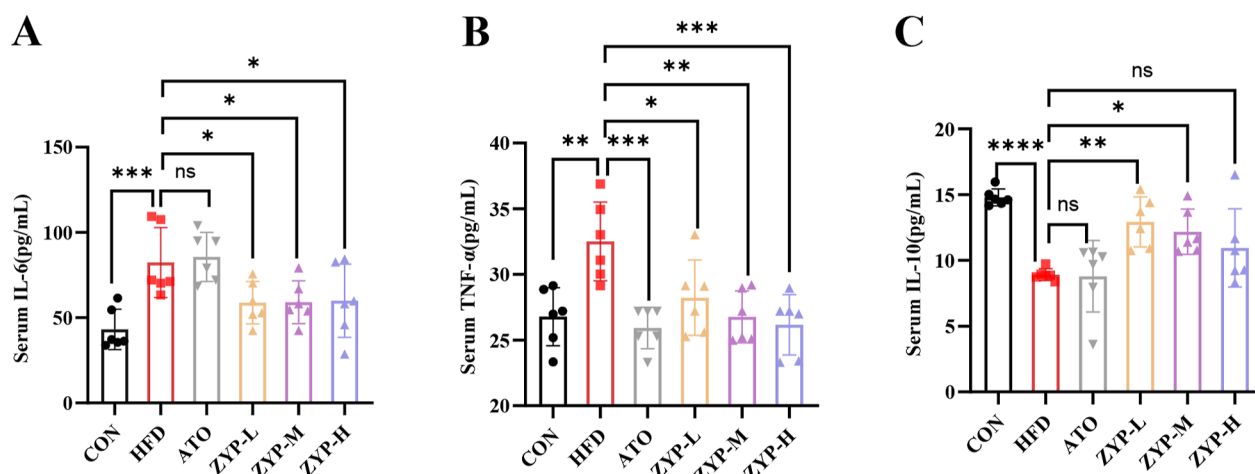
Figure 4. ZYP reduced inflammation in NAFLD mice. (A) Serum IL-6 levels. (B) Serum TNF-α levels. (C) Serum IL-10 levels. ****/***/**/*, $P < 0.0001/P < 0.001/P < 0.01/P < 0.05$; ns, not significant.

To identify metabolic alterations, PCA score plots were created using the identified fecal BAs. The separation trend between the CON, HFD, and ZYP-M groups is illustrated in Figure 6A,B. In Figure 6C, the specific changes in BA monomers are shown. BA concentrations in the feces of the CON group and the HFD group were quantitatively analyzed, and it was found that the HFD significantly increased levels of 12-ketolithocholic acid (12-KLCA), glycodeoxycholic acid (GDCA), chenodeoxycholic acid (CDCA), hyodeoxycholic acid (HDCA), apocholic acid (ApoCA), deoxycholic acid (DCA), isolithocholic acid (isoLCA), and lithocholic acid (LCA) and significantly decreased levels of taurochenodeoxycholic acid (TCDCA), tauromuricholic acid (TMCA), α-muricholic acid (α-MCA), and tauroursodeoxycholic acid (TUDCA) (Figure 6C). Compared with the HFD group, ZYP significantly increased levels of 7-KDCA, ursodeoxycholic acid (UDCA), cholic acid (CA), and glycocholic acid (GCA) and decreased levels of 12-KLCA, ApoCA, and isoLCA.

3.5. ZYP Alleviates NAFLD by Regulating BA Metabolism through FXR/FGF15 Signaling. To understand the mechanism behind changes in the BA profile brought on by ZYP, we also carried out mRNA analysis of hepatic and intestinal tissues to evaluate the expression of enzymes involved in BA production. The FXR receptor, which is abundantly expressed in the hepatic and intestinal organs, is known to be the main target of BA action. Intestinal FXR was found, and the HFD group's FXR mRNA expression was considerably higher than that of the CON group. However, compared to that in the HFD group, the expression of FXR mRNA was considerably downregulated in the ZYP-L and ZYP-M groups (Figure 7A). When we looked at FXR gene expression in the liver, we discovered that the HFD group had lower levels of FXR mRNA expression than the CON group did. In contrast, the ZYP-M and ZYP-H groups dramatically enhanced hepatic FXR mRNA expression in NAFLD mice (Figure 7E).

Additionally, we discovered that the ZYP treatment groups' intestinal FGF15 mRNA expression was different from that of the HFD group. The FGF15 gene in the intestine was significantly overexpressed in HFD mice, while the expression of FGF15 mRNA was dramatically reduced in the ZYP group (Figure 7B). The FGFR4 in the liver was significantly overexpressed in HFD mice, while FGFR4 expression was

significantly decreased in the ZYP treatment groups (Figure 7C). The current study shows that the intestinal FXR/FGF15 pathway is essential for downregulation of Cyp7a1 expression.[28] We examined the expression of Cyp7a1 mRNA in the liver and found that the expression of Cyp7a1 mRNA in the HFD group was significantly decreased, while it was significantly overexpressed in the ZYP treatment groups (Figure 7D).

Protein expression in hepatic and intestinal tissues was determined by western blotting. The results showed that compared with that in the CON group, the expression levels of FXR, FGF15 protein in the intestine and FGFR4 in the liver were increased, and the expression levels of Cyp7a1 and FXR protein in the liver were decreased in the HFD group. Compared with that in the HFD group, the expression levels of FXR and FGF15 protein in the intestine and FGFR4 protein in the liver were downregulated, while the expression levels of Cyp7a1 and FXR protein in the liver were upregulated in the ZYP treatment groups (Figure 8). These results were consistent with those of RT-qPCR.

4. DISCUSSION

NAFLD is a rapidly emerging and highly prevalent illness, which poses significant socioeconomic implications. TCM holds great potential in alleviating this health burden. In this study, we investigated the effects of ZYP on lipid levels, inflammatory factors, and fecal metabolomics in mice fed an HFD to mimic NAFLD. Our findings demonstrate that ZYP therapy effectively ameliorated NAFLD in HFD-fed mice, potentially through the upregulation of CYP7A1 via the intestinal FXR-FGF15 pathway, thereby modulating and improving BA metabolism.

NAFLD is primarily caused by an excess of lipids such as TC, TG, and LDL-C in the serum and/or liver, as well as a decrease in HDL-C, which often happens when the import of a significant number of lipids exceeds the clearance of hepatic lipids.[29] Our research findings demonstrate that ZYP, when administered to mice on an HFD, effectively reduces serum levels of TG, TC, and LDL-C, while simultaneously increasing HDL-C levels. Furthermore, the liver plays a crucial role in regulating lipid homeostasis, as well as glucose production and metabolism.[30] In our study, we observed that ZYP administration reduced blood glucose levels in mice fed an
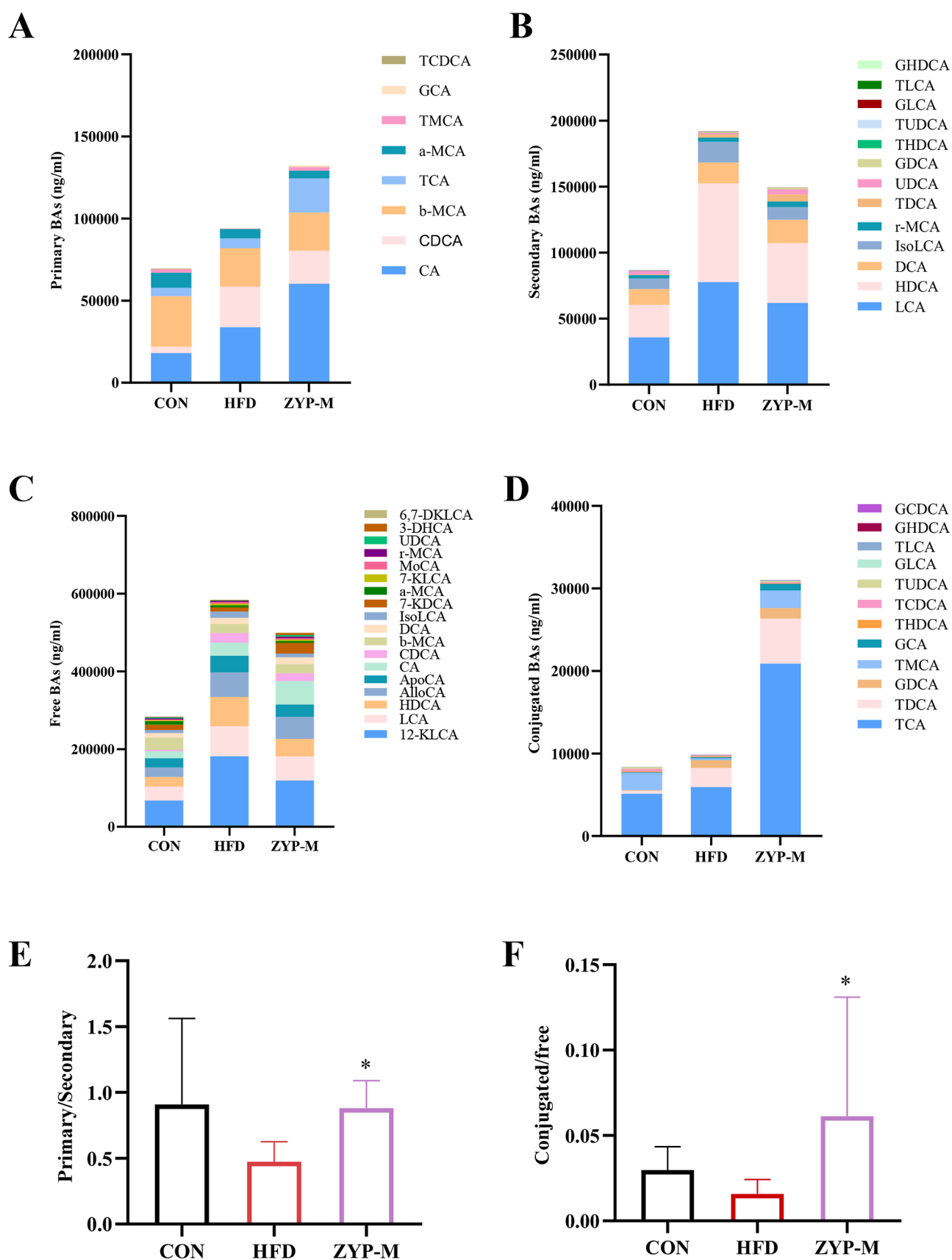
Figure 5. Effect of ZYP on different types of BAs in NAFLD mice. (A) Primary BA levels. (B) Secondary BA levels. (C) Free BA levels. (D) Conjugated BA levels. (E) Ratio of primary BAs to secondary BAs. (F) Ratio of conjugated BAs to free BAs. ****/***/**/*, $P < 0.0001/P < 0.001/P < 0.01/P < 0.05$; ns, not significant.
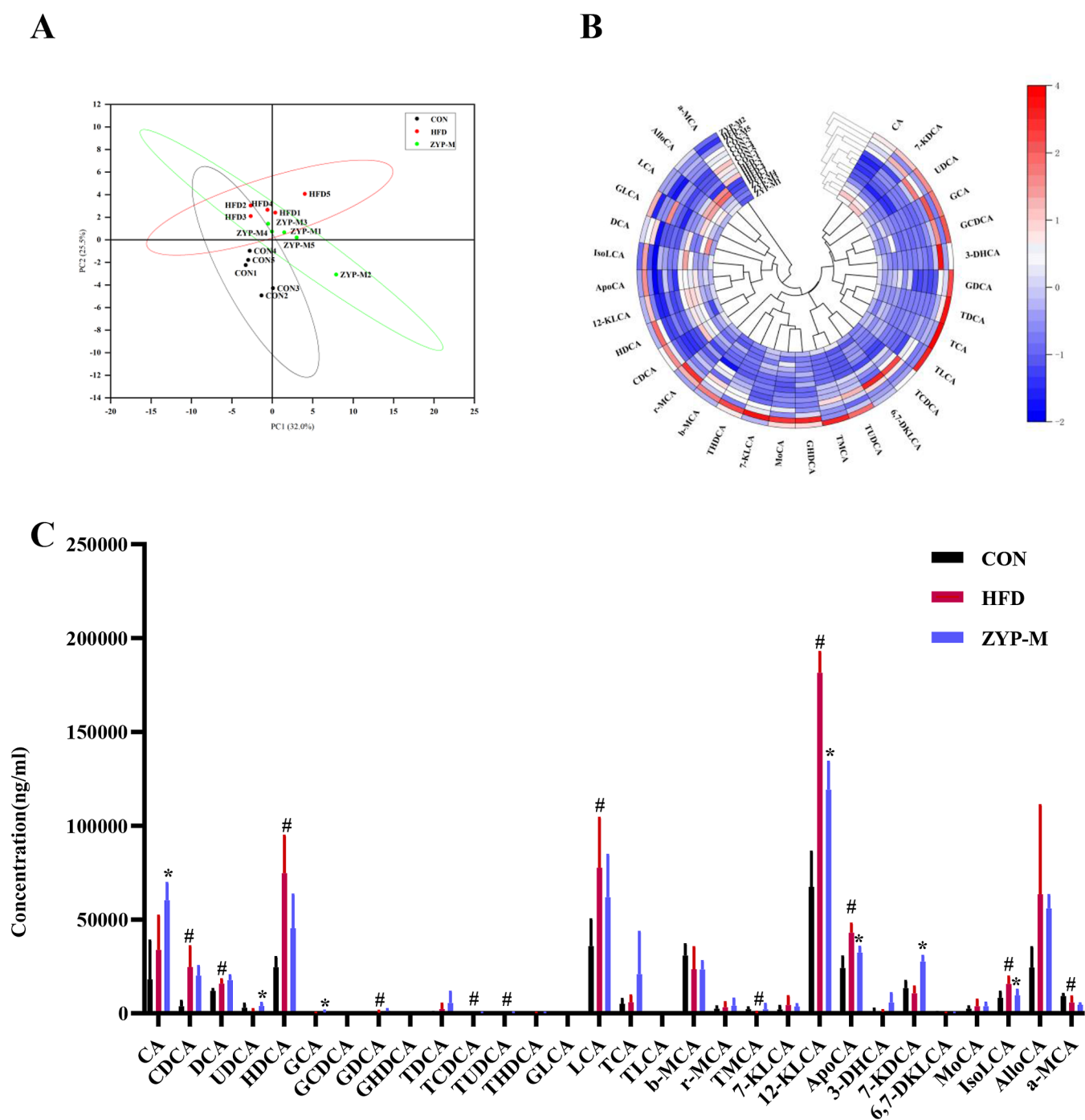
Figure 6. Effect of ZYP on fecal BA profiles. (A) PCA score plot. (B) Heat map. (C) Detailed changes in BA monomers. #$P < 0.05$, ##$P < 0.01$ compared with CON, *$P < 0.05$, and **$P < 0.01$ compared with HFD.

HFD. These findings indicate that ZYP has an impact on lipid and glucose synthesis. However, it is worth noting that the mice fed with an HFD showed a significant decrease in food intake and body weight, which could be attributed to the difference in taste between the HFD and the standard diet. Previous research has also highlighted that prolonged HFD feeding can lead to anorexia in animals, resulting in weight loss among experimental subjects.[31] The body weight of NAFLD mice was not significantly affected by ZYP, which aligns with our previous findings.[17]

The deposition of lipid droplets is a prominent characteristic in the early stage of NAFLD. Hepatic lipid deposition not only

contributes to the development of NAFLD but is also associated with type II diabetes, obesity, coronary athero-sclerotic heart disease, and other metabolic diseases.[32,33] The liver weight index of mice fed an HFD significantly increased. Additionally, the HFD group exhibited noticeable hepatic steatosis and ballooning hepatocyte degeneration. Treatment with ZYP significantly reduced the liver weight index and inhibited hepatic lipid deposition in HFD-fed mice, indicating a protective effect of ZYP on the liver of these mice.

In addition to adipocytes, adipose tissue also contains macrophages, which are closely linked to inflammation. Among the different types of inflammatory cells in the liver, the role of
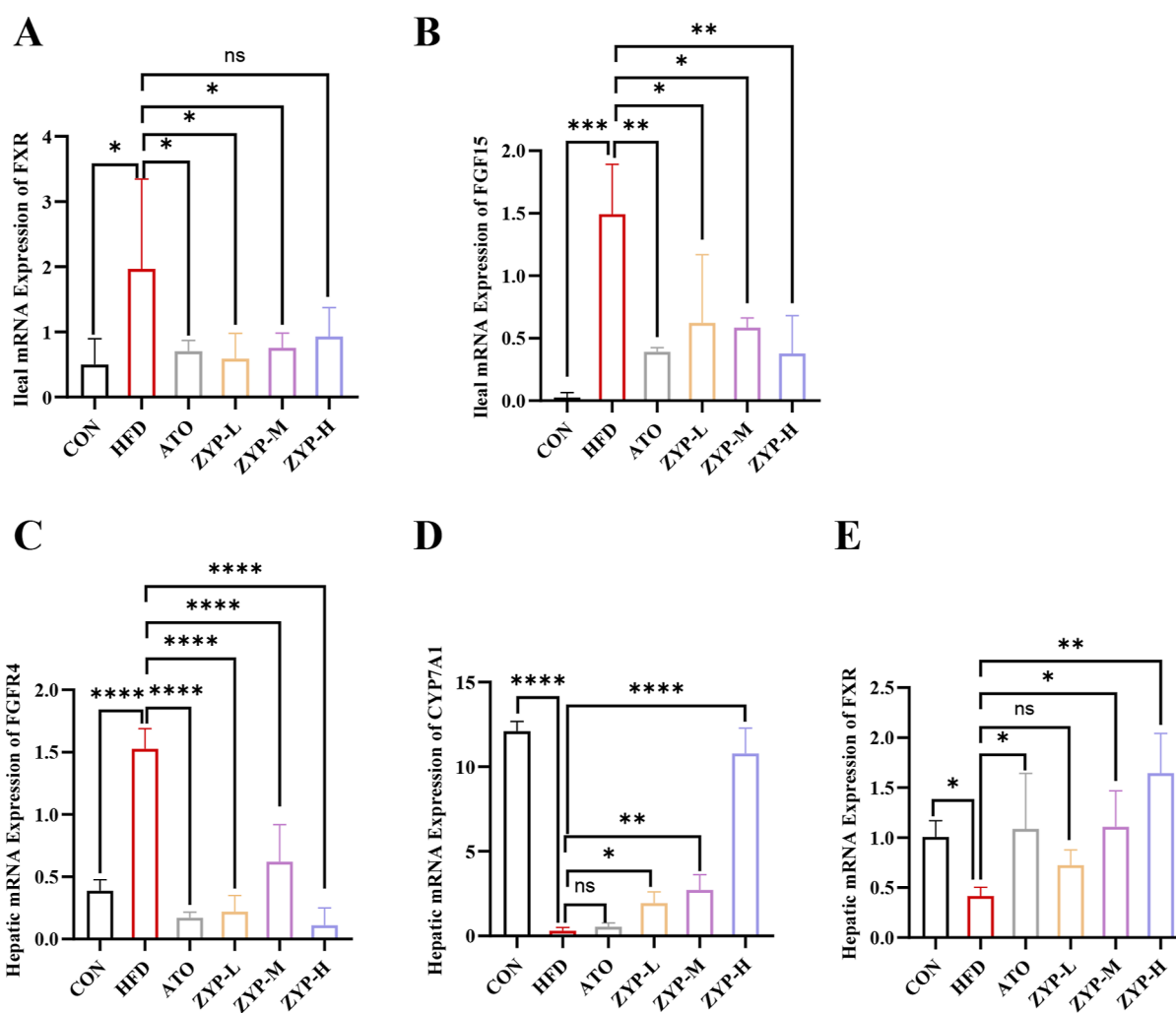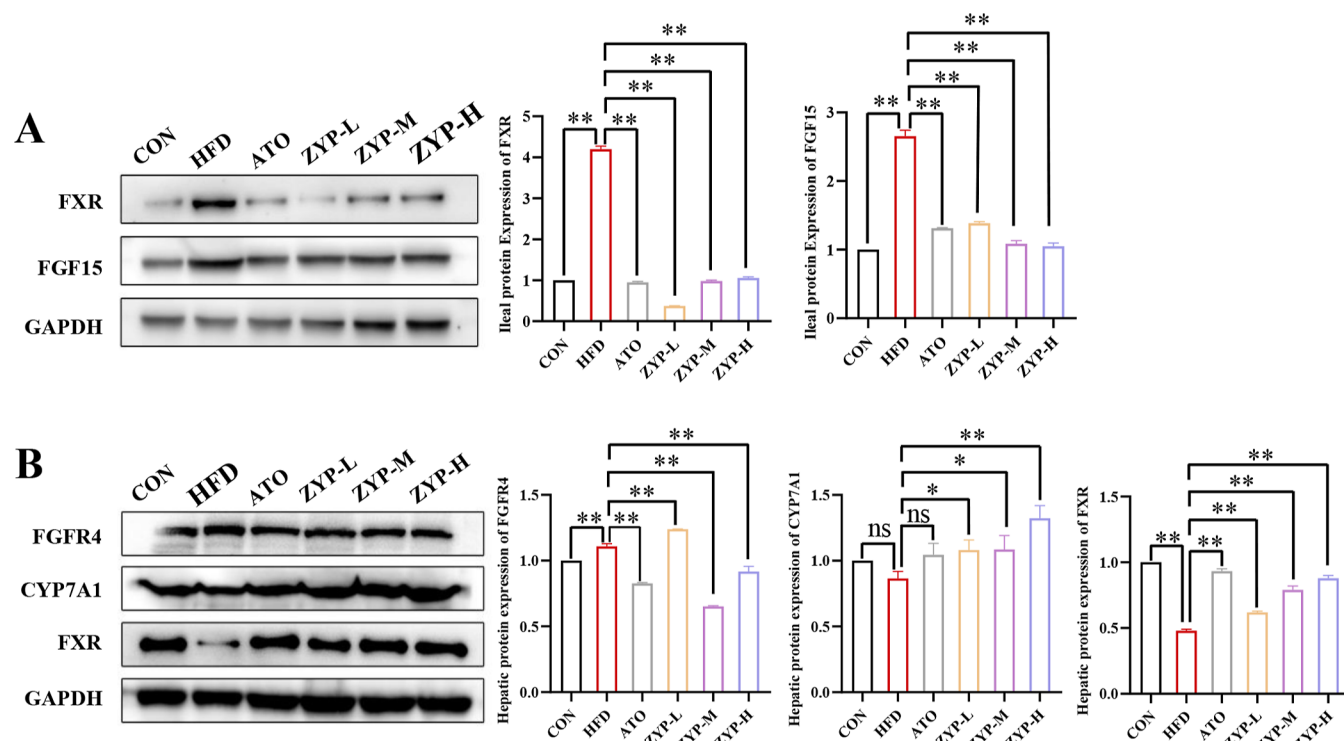
Figure 7. Relative mRNA expression of FXR-FGF15 members in HFD mice. (A) Relative mRNA expression levels of ileal FXR. (B) Relative mRNA expression levels of ileal FGF15. (C) Relative mRNA expression levels of hepatic FGFR4. (D) Relative protein expression levels of hepatic CYP7A1. (E) Relative protein expression levels of hepatic FXR. ****/***/**/*, $P < 0.0001/P < 0.001/P < 0.01/P < 0.05$; ns, not significant.

macrophages in the development of NAFLD has been extensively studied. Our investigation focused on assessing the impact of ZYP on inflammation. Macrophages are the primary immune cells responsible for releasing inflammatory cytokines, such as TNF-α and IL-6.[34] Our study demonstrated that ZYP administration reduced the levels of IL-6 and TNF-α in NAFLD mice. Furthermore, we observed that the increase in circulating IL-10 had an impact on serum TC levels.[35−37] Consistent with previous research, our findings indicated that serum IL-10 levels were significantly lower in HFD-fed mice than in the CON group, suggesting that long-term HFD reduced the content of IL-10.[38] However, in the ZYP group, the serum IL-10 content was significantly higher than that in the HFD group. These results suggest that ZYP exerts a protective effect on the liver by reducing HFD-induced inflammation.

BAs play a crucial role in clearing cholesterol and preventing the buildup of harmful substances, such as TG, cholesterol, and toxic compounds, which can cause damage to the liver and other organs.[39] Additionally, BAs also function as signaling molecules that regulate metabolism and inflammation and contribute to the inflammatory response in both liver and other tissues.[40] In our study, we analyzed fecal samples to investigate changes in the profile of BA metabolites. Our

findings revealed that ZYP treatment increased the levels of primary BAs and conjugated BAs while reducing the levels of secondary BAs and free BAs in the fecal BA profile of mice fed an HFD. Primary BAs are produced via the CYP7A1-mediated classical pathway or the CYP27A1-mediated alternative pathway from cholesterol. Conjugated BAs are formed by combining primary BAs with taurine and glycine or free BAs reabsorbed in the intestine, return to the liver through the portal vein, and synthesize conjugated BAs under the action of liver cells. BAs are discharged into the small intestine by the organism during digestion to complete lipid absorption. To complete the enterohepatic circulation of BAs, the bound BAs are dehydroxylated to create secondary BAs, which are reabsorbed back into the liver via the portal system. ZYP is thought to play a role by promoting BA synthesis and decreasing BA reabsorption.

The changes in the classical and alternative BA synthesis routes in the liver can be observed through the CA/CDCA ratio.[41] ZYP increases the level of CA while decreasing the content of CDCA, which may impact BA synthesis by acting on the CYP7A1-mediated classical synthesis route. In individuals with NASH and clinically significant fibrosis, the content of 12KLCA, LCA, DCA, and many BAs generated from DCA (e.g., GDCA, TDCA, etc.) increased with disease

Figure 8. Relative protein expression of FXR-FGF15 members in HFD mice. (A) Relative protein expression levels of ileal FXR and FGF15. (B) Relative protein expression levels of hepatic FGFR4, CYP7A1, and FXR. ****/***/**/*, $P < 0.0001/P < 0.001/P < 0.01/P < 0.05$; ns, not significant.

activity and fibrosis.[42,43] In line with the findings of this investigation, our findings revealed that the levels of 12KLCA, LCA, DCA, and GDCA in the fecal BAs of mice in the HFD group were elevated. TCDCA, TUDCA, UDCA, and 7-KDCA are FXR antagonists that inhibit intestinal FXR signaling, decrease FGF15 expression in the ileum, and enhance CYP7A1 expression in the liver.[44] TUDCA and TCDCA were dramatically downregulated in the HFD group, but ZYP increased UDCA and 7-KDCA, so we speculated that ZYP might inhibit the intestinal FXR signaling pathway by regulating the above specific BAs.

We explored whether the effect of ZYP on BA synthesis was mediated through FXR because FXR is known to play a vital role in regulating BA production and homeostasis. The therapeutic efficacy of ZYP on NAFLD was confirmed by RT-qPCR and western blot, which showed that it suppresses the intestinal FXR-FGF15 signaling and increases the expression of CYP7A1 to stimulate the synthesis of BAs. Research has shown that HFD feeding dramatically increases the levels of TC and TG in CYP7A1$^{-/-}$ mice.[45] Similar results were observed in our investigation, where compared to that in the CON group, the expression of CYP7A1 in the liver of the HFD group was downregulated, while serum levels of TC, TG, and LDL-C were increased. We found that ZYP therapy overexpressed CYP7A1 in the liver while decreasing serum TC, TG, and LDL-C levels. CYP7A1 converts excess cholesterol into BA, reducing cholesterol accumulation.[46] As a result, our findings indicated that ZYP increased the synthesis of BA and decreased lipid levels by upregulating the expression of CYP7A1.

FXR is extensively expressed in both the intestine and the liver, and the data demonstrate that the intestinal FXR/FGF15 pathway regulates CYP7A1 more strongly.[47,48] BA synthesis

was found to be increased in intestine-specific FXR$^{-/-}$ mice.[49] FGF15$^{-/-}$ mice have enhanced CYP7A1 expression and BA synthesis.[50] According to a recent study, HFD eating activates the intestinal FXR-FGF15 pathway in mice, inhibits hepatic CYP7A1 transcription, lowers cholesterol clearance, and eventually leads to hepatic cholesterol accumulation.[51] In this work, ZYP therapy blocked FXR/FGF15 pathway activation, resulting in enhanced CYP7A1 expression and BA production. Furthermore, for FGFR4, another important receptor in the FXR-FGF15 pathway, our findings demonstrated that ZYP dramatically reduced FGFR4 expression. FGFR4 was found to be upregulated in NASH model mice and fatty liver-associated HCC patients.[52,53] In vitro, investigations have indicated that inhibiting FGFR4 activation prevents steatosis and the formation of fatty liver in mice.[54] Many studies have shown that the FXR/FGF15 axis plays a crucial role in BA control. For example, chlorogenic acid promotes metabolic clearance of cholesterol by blocking the FXR-FGF15 pathway.[41] Similarly, L-theanine intervention produced low FXR and FGF15 expression and high CYP7A1 expression, reduced TC, TG, and LDL-C content, increased HDL-C content, and improved lipid metabolism.[55] Nuciferine changes the composition of colonic BA, increases the level of conjugated Bas, inhibits ileal FXR signal transduction, upregulates the expression of CYP7A1, promotes BA synthesis, inhibits BA reabsorption, and promotes fecal BA excretion, thereby alleviating NAFLD.[56]

The hepatic FXR-liver X receptor α (LXRα) pathway and the intestinal FXR-FGF15 pathway work together in the synthesis of BA.[57] Our previous research has shown that berberine and evodiamine, the main active ingredient of ZYP, effectively increase the expression of LXRα and CYP7A1.[58] Activation of LXRα stimulates the transcription of CYP7A1,

indirectly promoting the conversion of cholesterol into BAs.[59] In this work, it was observed that animals fed an HFD had higher levels of TC, TG, and LDL-C. This was due to an upregulation of intestinal FXR expression and a downregulation of liver FXR expression. However, when ZYP was administered to HFD-fed mice, it increased FXR expression in the liver and decreased FXR activity in the intestine, resulting in lower levels of TC, TG, and LDL-C. Therefore, the cholesterol-lowering effect of ZYP is achieved through a combination of reducing the intestinal FXR-FGF15 pathway and increasing the hepatic FXR pathway. These findings are consistent with those of another investigation in which theabrownin increased hepatic FXR but decreased intestinal FXR due to a significant buildup of taurine-bound BA in the distal ileum[60] It demonstrates that TCM treatment of NAFLD has multi-target, multi-channel, and overall coordination properties.

5. CONCLUSIONS

In conclusion, ZYP intervention improved HFD-induced NAFLD, and the underlying mechanisms may include the following: (1) improved inflammatory response, (2) increased primary BA biosynthesis, (3) increased conjugated BAs, especially UDCA and 7-KDCA, which act antagonistically on intestinal FXR, and (4) reduced activity of intestinal FXR, resulting in decreased expression of FGF15, followed by decreased activation of the FGF15-FGFR4 pathway and increased expression of CYP7A1. We demonstrated the efficacy of ZYP in the treatment of NAFLD and elucidated the mechanism of action, which is a potential therapeutic option for the treatment of NAFLD in the clinic.

■ ASSOCIATED CONTENT

ⓢ Supporting Information

The Supporting Information is available free of charge at https://pubs.acs.org/doi/10.1021/acsomega.3c01955.

Initial body weight and serum TC levels (PDF)

■ AUTHOR INFORMATION

Corresponding Authors

Xin Zhou — *School of Basic Medicine, Chengdu University of Traditional Chinese Medicine, Chengdu 611137, China;* Email: zhouxin@cdutcm.edu.cn

Tao Shen — *School of Basic Medicine, Chengdu University of Traditional Chinese Medicine, Chengdu 611137, China;* Email: st@cdutcm.edu.cn

Authors

Lu Xu — *School of Traditional Chinese Medicine, Jinan University, Guangzhou, Guangdong 510632, China;* ⓞ orcid.org/0009-0004-7198-3072

Kunhe Xu — *School of Basic Medicine, Chengdu University of Traditional Chinese Medicine, Chengdu 611137, China*

Peiyu Xiong — *School of Basic Medicine, Chengdu University of Traditional Chinese Medicine, Chengdu 611137, China*

Chun Zhong — *Sichuan Second Hospital of Traditional Chinese Medicine, Chengdu 610014, China*

Xiaobo Zhang — *School of Basic Medicine, Chengdu University of Traditional Chinese Medicine, Chengdu 611137, China;* ⓞ orcid.org/0000-0002-9916-3832

Rui Gao — *School of Basic Medicine, Chengdu University of Traditional Chinese Medicine, Chengdu 611137, China*

Complete contact information is available at:
https://pubs.acs.org/10.1021/acsomega.3c01955

■ REFERENCES

(1) Younossi, Z. M. Non-alcoholic fatty liver disease—a global public health perspective. *J. Hepatol.* **2019**, *70*, 531−544.

(2) Younossi, Z.; Anstee, Q. M.; Marietti, M.; Hardy, T.; Henry, L.; Eslam, M.; George, J.; Bugianesi, E. Global burden of NAFLD and NASH: trends, predictions, risk factors and prevention. *Nat. Rev. Gastroenterol. Hepatol.* **2018**, *15*, 11−20.

(3) Tilg, H.; Adolph, T. E.; Dudek, M.; Knolle, P. Non-alcoholic fatty liver disease: the interplay between metabolism, microbes and immunity. *Nat. Metab.* **2021**, *3*, 1596−1607.

(4) Younossi, Z. M.; Blissett, D.; Blissett, R.; Henry, L.; Stepanova, M.; Younossi, Y.; Racila, A.; Hunt, S.; Beckerman, R. The economic and clinical burden of nonalcoholic fatty liver disease in the United States and Europe. *Hepatology* **2016**, *64*, 1577−1586.

(5) Powell, E. E.; Wong, V. W. S.; Rinella, M. Non-alcoholic fatty liver disease. *Lancet.* **2021**, *397*, 2212−2224.

(6) Sheka, A. C.; Adeyi, O.; Thompson, J.; Hameed, B.; Crawford, P. A.; Ikramuddin, S. Nonalcoholic steatohepatitis: a review. *JAMA* **2020**, *323*, 1175−1183.

(7) Diehl, A. M.; Day, C. Cause, pathogenesis, and treatment of nonalcoholic steatohepatitis. *N. Engl. J. Med.* **2017**, *377*, 2063−2072.

(8) Ferguson, D.; Finck, B. N. Emerging therapeutic approaches for the treatment of NAFLD and type 2 diabetes mellitus. *Nat. Rev. Endocrinol.* **2021**, *17*, 484−495.

(9) Stahl, E. P.; Dhindsa, D. S.; Lee, S. K.; Sandesara, P. B.; Chalasani, N. P.; Sperling, L. S. Nonalcoholic fatty liver disease and the heart: JACC state-of-the-art review. *J Am Coll Cardiol.* **2019**, *73*, 948−963.

(10) Pan, J.; Wang, M.; Song, H.; Wang, L.; Ji, G. The efficacy and safety of traditional chinese medicine (jiang zhi granule) for nonalcoholic Fatty liver: a multicenter, randomized, placebo-controlled study. *J. Evidence-Based Complementary Altern. Med.* **2013**, *2013*, 1−8.

(11) Shi, T.; Wu, L.; Ma, W.; Ju, L.; Bai, M.; Chen, X.; Liu, S.; Yang, X.; Shi, J. Nonalcoholic fatty liver disease: pathogenesis and treatment in traditional chinese medicine and western medicine. *J. Evidence-Based Complementary Altern. Med.* **2020**, *2020*, 1−16.

(12) Liu, C.; Liao, J. Z.; Li, P. Y. Traditional Chinese herbal extracts inducing autophagy as a novel approach in therapy of nonalcoholic fatty liver disease. *World J. Gastroenterol.* **2017**, *23*, 1964−1973.

(13) Guo, W.; Huang, J.; Wang, N.; Tan, H. Y.; Cheung, F.; Chen, F.; Feng, Y. Integrating Network Pharmacology and Pharmacological Evaluation for Deciphering the Action Mechanism of Herbal Formula Zuojin Pill in Suppressing Hepatocellular Carcinoma. *Front. Pharmacol.* **2019**, *10*, 1185.

(14) Li, Y. Y.; Feng, J. L.; Li, Z.; Zang, X. Y.; Yang, X. W. Separation and Enrichment of Alkaloids from Coptidis Rhizoma and Euodiae Fructus by Macroporous Resin and Evaluation of the Effect on Bile Reflux Gastritis Rats. *Molecules* **2022**, *27*, 724.

(15) Wang, R.; Wang, Y.; Lu, Z.; Jing, J.; Wang, Z.; He, T.; Tian, M.; Yuan, Z.; Cui, Y.; Rong, W.; et al. Efficacy and Safety of Zuojin Pill for the Treatment of Chronic Nonatrophic Gastritis: A Randomized Active-Controlled Clinical Trial. *J. Evidence-Based Complementary Altern. Med.* **2022**, *2022*, 1−9.

(16) Hu, S.; Wei, P.; Li, W.; Liu, Q.; Chen, S.; Hu, C.; Guo, X.; Ma, X.; Zeng, J.; Zhang, Y. Pharmacological effects of berberine on models of ulcerative colitis: A meta-analysis and systematic review of animal studies. *Front. Pharmacol.* **2022**, *13*, 937029.

(17) Zhou, X.; Ren, F.; Wei, H.; Liu, L.; Shen, T.; Xu, S.; Wei, J.; Ren, J.; Ni, H. Combination of berberine and evodiamine inhibits intestinal cholesterol absorption in high fat diet induced hyperlipidemic rats. *Lipids Health Dis.* **2017**, *16*, 239.

(18) Mai, W.; Xu, Y.; Xu, J.; Zhao, D.; Ye, L.; Yu, G.; Wang, Z.; Lu, Q.; Lin, J.; Yang, T.; et al. Berberine Inhibits Nod-Like Receptor Family Pyrin Domain Containing 3 Inflammasome Activation and Pyroptosis in Nonalcoholic Steatohepatitis via the ROS/TXNIP Axis. *Front. Pharmacol.* **2020**, *11*, 185.

(19) Zhang, X.; Gao, R.; Zhou, Z.; Sun, J.; Tang, X.; Li, J.; Zhou, X.; Shen, T. Uncovering the mechanism of Huanglian-Wuzhuyu herb pair in treating nonalcoholic steatohepatitis based on network pharmacology and experimental validation. *J. Ethnopharmacol.* **2022**, *296*, 115405.

(20) Yu, H.; Liu, C.; Zhang, F.; Wang, J.; Han, J.; Zhou, X.; Wen, Y.; Shen, T. Efficacy of Zhuyu Pill Intervention in a Cholestasis Rat Model: Mutual Effects on Fecal Metabolism and Microbial Diversity. *Front. Pharmacol.* **2021**, *12*, 695035.

(21) Yu, H.; Liu, C.; Wang, J.; Han, J.; Zhang, F.; Zhou, X.; Wen, Y.; Shen, T. miRNA and miRNA target genes in intervention effect of Zhuyu pill on cholestatic rat model. *J. Ethnopharmacol.* **2022**, *283*, 114709.

(22) Ahmad, T. R.; Haeusler, R. A. Bile acids in glucose metabolism and insulin signalling - mechanisms and research needs. *Nat. Rev. Endocrinol.* **2019**, *15*, 701−712.

(23) Inagaki, T.; Choi, M.; Moschetta, A.; Peng, L.; Cummins, C. L.; McDonald, J. G.; Luo, G.; Jones, S. A.; Goodwin, B.; Richardson, J. A.; et al. Fibroblast growth factor 15 functions as an enterohepatic signal to regulate bile acid homeostasis. *Cell Metab.* **2005**, *2*, 217−225.

(24) Hagel, M.; Miduturu, C.; Sheets, M.; Rubin, N.; Weng, W.; Stransky, N.; Bifulco, N.; Kim, J. L.; Hodous, B.; Brooijmans, N.; et al. First Selective Small Molecule Inhibitor of FGFR4 for the Treatment of Hepatocellular Carcinomas with an Activated FGFR4 Signaling Pathway. *Cancer Discovery* **2015**, *5*, 424−437.

(25) Liu, W. Y.; Xie, D. M.; Zhu, G. Q.; Huang, G. Q.; Lin, Y. Q.; Wang, L. R.; Shi, K. Q.; Hu, B.; Braddock, M.; Chen, Y. P.; et al. Targeting fibroblast growth factor 19 in liver disease: a potential biomarker and therapeutic target. *Expert Opin. Ther. Targets* **2015**, *19*, 675.

(26) Luo, M.; Yan, J.; Wu, L.; Wu, J.; Chen, Z.; Jiang, J.; Chen, Z.; He, B. Probiotics Alleviated Nonalcoholic Fatty Liver Disease in High-Fat Diet-Fed Rats via Gut Microbiota/FXR/FGF15 Signaling Pathway. *J. Immunol. Res.* **2021**, *2021*, 1−10.

(27) Zhang, Q.; Wang, G. j.; A, J. y.; Wu, D.; Zhu, L. l.; Ma, B.; Du, Y. Application of GC/MS-based metabonomic profiling in studying the lipid-regulating effects of Ginkgo Biloba extract on diet-induced hyperlipidemia in rats. *Acta Pharmacol. Sin.* **2009**, *30*, 1674.

(28) Zaborska, K. E.; Cummings, B. P. Rethinking bile acid metabolism and signaling for type 2 diabetes treatment. *Curr. Diabetes Rep.* **2018**, *18*, 109.

(29) Lambert, J. E.; Ramos−Roman, M. A.; Browning, J. D.; Parks, E. J. Increased De novo lipogenesis is a distinct characteristic of individuals with nonalcoholic fatty liver disease. *Gastroenterology* **2014**, *146*, 726.

(30) Trefts, E.; Gannon, M.; Wasserman, D. H. The liver. *Curr. Biol.* **2017**, *27*, R1147−R1151.

(31) Zhu, J.; Zhao, J.; Qin, W.; Song, D.; Bao, Y.; Liu, H.; et al. The Animal Models of Hyperlipidemia: A Review. *Lab. Anim. Sci.* **2012**, *2*, 48−52.

(32) Ullah, R.; Rauf, N.; Nabi, G.; Ullah, H.; Shen, Y.; Zhou, Y. D.; Fu, J. Role of nutrition in the pathogenesis and prevention of nonalcoholic fatty liver disease: recent updates. *Int. J. Biol. Sci.* **2019**, *15*, 265−276.

(33) Li, X.; Cui, K.; Fang, W.; Chen, Q.; Xu, D.; Mai, K.; Zhang, Y.; Ai, Q. High level of dietary olive oil decreased growth, increased liver lipid deposition and induced inflammation by activating the p38 MAPK and JNK pathways in large yellow croaker (Larimichthys crocea). *Fish Shellfish Immunol.* **2019**, *94*, 157−165.

(34) Zhang, L.; Wang, C. C. Inflammatory response of macrophages in infection. *Hepatobiliary Pancreatic Dis. Int.* **2014**, *13*, 138−152.

(35) Von Der Thüsen, J. H.; Kuiper, J.; Fekkes, M. L.; De Vos, P.; Van Berkel, T. J. C.; Biessen, E. A. L. Attenuation of atherogenesis by systemic and local adenovirus-mediated gene transfer of interleukin-10 in LDLr-/- mice. *FASEB J.* **2001**, *15*, 1−19.

(36) Yoshioka, T.; Okada, T.; Maeda, Y.; Ikeda, U.; Shimpo, M.; Nomoto, T.; Takeuchi, K.; Nonaka-Sarukawa, M.; Ito, T.; Takahashi, M.; et al. Adeno-associated virus vector-mediated interleukin-10 gene transfer inhibits atherosclerosis in apolipoprotein E-deficient mice. *Gene Ther.* **2004**, *11*, 1772−1779.

(37) Liu, Y.; Li, D.; Chen, J.; Xie, J.; Bandyopadhyay, S.; Zhang, D.; Nemarkommula, A. R.; Liu, H.; Mehta, J. L.; Hermonat, P. L. Inhibition of atherogenesis in LDLR knockout mice by systemic delivery of adeno-associated virus type 2-hIL-10. *Atherosclerosis* **2006**, *188*, 19−27.

(38) Schaalan, M. F.; Ramadan, B. K.; Abd Elwahab, A. H. Synergistic effect of carnosine on browning of adipose tissue in exercised obese rats; a focus on circulating irisin levels. *J. Cell. Physiol.* **2018**, *233*, 5044−5057.

(39) Chiang, J. Y. L.; Ferrell, J. M. Bile acids as metabolic regulators and nutrient sensors. *Annu. Rev. Nutr.* **2019**, *39*, 175−200.

(40) Bing, H.; Li, Y. L. The role of bile acid metabolism in the occurrence and development of NAFLD. *Front. Mol. Biosci.* **2022**, *9*, 1089359.

(41) Ye, X.; Li, J.; Gao, Z.; Wang, D.; Wang, H.; Wu, J. Chlorogenic Acid Inhibits Lipid Deposition by Regulating the Enterohepatic FXR-FGF15 Pathway. *BioMed Res. Int.* **2022**, *2022*, 1−11.

(42) Loomba, R.; Noureddin, M.; Kowdley, K. V.; Kohli, A.; Sheikh, A.; Neff, G.; Bhandari, B. R.; Gunn, N.; Caldwell, S. H.; Goodman, Z.; et al. Combination therapies including Cilofexor and Firsocostat for bridging fibrosis and cirrhosis attributable to NASH. *Hepatology* **2021**, *73*, 625−643.

(43) Muthiah, M. D.; Smirnova, E.; Puri, P.; Chalasani, N.; Shah, V. H.; Kiani, C.; Taylor, S.; Mirshahi, F.; Sanyal, A. J. Development of alcohol-associated hepatitis is associated with specific changes in gut-modified bile acids. *Hepatol. Commun.* **2022**, *6*, 1073−1089.

(44) Zhao, L.; Yang, W.; Chen, Y.; Huang, F.; Lu, L.; Lin, C.; Huang, T.; Ning, Z.; Zhai, L.; Zhong, L. L.; et al. A Clostridia-rich microbiota enhances bile acid excretion in diarrhea-predominant irritable bowel syndrome. *J. Clin. Invest.* **2020**, *130*, 438−450.

(45) Chen, J. Y.; Levy-Wilson, B.; Goodart, S.; Cooper, A. D. Mice expressing the human CYP7A1 gene in the mouse CYP7A1 knock-out background lack induction of CYP7A1 expression by cholesterol feeding and have increased hypercholesterolemia when fed a high fat diet. *J. Biol. Chem.* **2002**, *277*, 42588−42595.

(46) Liu, H.; Pathak, P.; Boehme, S.; Chiang, J. Cholesterol 7α-hydroxylase protects the liver from inflammation and fibrosis by maintaining cholesterol homeostasis. *J. Lipid Res.* **2016**, *57*, 1831−1844.

(47) Qin, J.; Li, Y.; Cai, Z.; Li, S.; Zhu, J.; Zhang, F.; Liang, S.; Zhang, W.; Guan, Y.; Shen, D.; et al. A metagenome-wide association study of gut microbiota in type 2 diabetes. *Nature* **2012**, *490*, 55−60.

(48) Kim, I.; Ahn, S. H.; Inagaki, T.; Choi, M.; Ito, S.; Guo, G. L.; Kliewer, S. A.; Gonzalez, F. J. Differential regulation of bile acid homeostasis by the farnesoid X receptor in liver and intestine. *J. Lipid Res.* **2007**, *48*, 2664.

(49) Sun, R.; Yang, N.; Kong, B.; Cao, B.; Feng, D.; Yu, X.; Ge, C.; Huang, J.; Shen, J.; Wang, P.; et al. Orally administered berberine modulates hepatic lipid metabolism by altering microbial bile acid metabolism and the intestinal FXR signaling pathway. *Mol. Pharmacol.* **2017**, *91*, 110−122.

(50) Kim, Y. C.; Byun, S.; Seok, S.; Guo, G.; Xu, H. E.; Kemper, B.; Kemper, J. K. Small heterodimer partner and fibroblast growth factor 19 inhibit expression of NPC1L1 in mouse intestine and cholesterol absorption. *Gastroenterology* **2019**, *156*, 1052−1065.

(51) Duan, Y.; Zhang, F.; Yuan, W.; Wei, Y.; Wei, M.; Zhou, Y.; Yang, Y.; Chang, Y.; Wu, X. Hepatic cholesterol accumulation ascribed to the activation of ileum Fxr-Fgf15 pathway inhibiting hepatic Cyp7a1 in high-fat diet-induced obesity rats. *Life Sci.* **2019**, *232*, 116638.

(52) Cui, G.; Martin, R. C.; Jin, H.; Liu, X.; Pandit, H.; Zhao, H.; Cai, L.; Zhang, P.; Li, W.; Li, Y. Up-regulation of FGF15/19 signaling promotes hepatocellular carcinoma in the background of fatty liver. *J. Exp. Clin. Cancer Res.* **2018**, *37*, 136.

(53) Li, Y.; Zhang, W.; Doughtie, A.; Cui, G.; Li, X.; Pandit, H.; Yang, Y.; Li, S.; Martin, R. Up-regulation of fibroblast growth factor 19 and its receptor associates with progression from fatty liver to hepatocellular carcinoma. *Oncotarget* **2016**, *7*, 52329−52339.

(54) Chen, Q.; Jiang, Y.; An, Y.; Zhao, N.; Zhao, Y.; Yu, C. Soluble FGFR4 extracellular domain inhibits FGF19-induced activation of FGFR4 signaling and prevents nonalcoholic fatty liver disease. *Biochem. Biophys. Res. Commun.* **2011**, *409*, 651−656.

(55) Xu, W.; Kong, Y.; Zhang, T.; Gong, Z.; Xiao, W. L-Theanine regulates lipid metabolism by modulating gut microbiota and bile acid metabolism. *J. Sci. Food Agric.* **2022**, *103*, 1283−1293.

(56) Sun, J.; Fan, J.; Li, T.; Yan, X.; Jiang, Y. Nuciferine Protects Against High-Fat Diet-Induced Hepatic Steatosis via Modulation of Gut Microbiota and Bile Acid Metabolism in Rats. *J. Agric. Food Chem.* **2022**, *70*, 12014−12028.

(57) Calkin, A. C.; Tontonoz, P. Transcriptional integration of metabolism by the nuclear sterol-activated receptors LXR and FXR. *Nat. Rev. Mol. Cell Biol.* **2012**, *13*, 213−224.

(58) Wei, H.; Lin, J. J.; Wang, J.; Shen, T. Antihyperlipidemic effect of a combination of berberine and evodiamine and its role in upregulating the protein expression of liver X receptor alpha and peroxisome proliferator-activated receptor gamma (in Chinese). *J. Hunan Univ. Chin. Med.* **2017**, *33*, 126−129.

(59) Lehmann, J. M.; Kliewer, S. A.; Moore, L. B.; Smith-Oliver, T. A.; Oliver, B. B.; Su, J. L.; Sundseth, S. S.; Winegar, D. A.; Blanchard, D. E.; Spencer, T. A.; et al. Activation of the nuclear receptor LXR by oxysterols defines a new hormone response pathway. *J. Biol. Chem.* **1997**, *272*, 3137.

(60) Huang, F.; Zheng, X.; Ma, X.; Jiang, R.; Zhou, W.; Zhou, S.; Zhang, Y.; Lei, S.; Wang, S.; Kuang, J.; et al. Theabrownin from Pu-erh tea attenuates hypercholesterolemia via modulation of gut microbiota and bile acid metabolism. *Nat. Commun.* **2019**, *10*, 4971.